Eur. Phys. J. A **21**, 303–312 (2004)
DOI 10.1140/epja/i2003-10207-y

THE EUROPEAN PHYSICAL JOURNAL A

The study of the neutral pion production in proton-proton collisions at beam momenta 1581 and 1683 MeV/c

V.V. Sarantsev[a], K.N. Ermakov, V.I. Medvedev, T.S. Oposhnyan, O.V. Rogachevsky, and S.G. Sherman

Petersburg Nuclear Physics Institute, Gatchina 188300, Russia

Received: 15 December 2003 / Revised version: 23 January 2004 /
Published online: 10 August 2004 –
Communicated by V.V. Anisovich

Abstract. The detailed investigation of the reaction $pp \to pp\pi^0$ has been carried out at two incident proton momenta. Momentum, angular and effective-mass distributions were analyzed in the framework of the one-pion exchange model. Taking into account only the P_{33}-wave in the pole diagrams allows one to obtain a good agreement with experimental data on differential distributions. At the same time the predictions for total cross-sections are much lower than the experimental data.

PACS. 13.75.Cs Nucleon-nucleon interactions (including antinucleons, deuterons, etc.) – 13.85.Lg Total cross-sections – 25.40.Ep Inelastic proton scattering

1 Introduction

The pion production in the NN interactions is the main inelastic process at the energies below 1 GeV. Despite the fact that a lot of experiments have been performed, many questions on this process are not yet answered. One of them is the question of the contribution of the isoscalar ($I = 0$) channel to the inelastic neutron-proton collisions. Since the neutron-proton scattering amplitude contains both isoscalar and isovector ($I = 1$) parts, a detailed investigation of the neutral pion production in the pp collisions (isovector contribution only) might give the most accurate information on the isovector channel that, in a combination with the neutron-proton data, would allow one to extract more correctly the contribution of the isoscalar channel.

Various theoretical models, more or less successful, arose while the data on the pion production in NN collisions were accumulated. Most of them work for pion production near the production threshold and are not applied at higher energies.

For the energy range 1–3 GeV an earlier peripheral or one-pion exchange (OPE) model [1] assumed the dominance of the one-pion exchange term in the inelastic amplitude. Pole diagram matrix elements were calculated using the uncertain beforehand form factor, the interference between diagrams being neglected. The form factor function was obtained then by fitting to experimental data, so, in fact, this was a semiphenomenological model. Its predictions were in a good agreement with rather rough measurements of the differential cross-sections in the energy range 800–1300 MeV. It was one of the reasons why both theoretical and experimental investigations in this energy range were not very popular.

The situation changed when the structures were observed in the energy dependence of the difference of the proton-proton total cross-sections for pure spin states, $\Delta\sigma_L$ and $\Delta\sigma_T$ [2]. One of the intriguing possible explanations of these structures was the hypothesis of the dibaryon resonances. Intensive investigations in this field enriched considerably both the theory of the pion production and experimental data, though the status of these dibaryons is not clarified yet (for a recent review, see [3]).

After the papers [4–6] it became evident that the modifications of the one-pion exchange model used there describe rather well (with the accuracy of 5–10%) the differential spectra for the $pp \to pn\pi^+$ reaction which provided the largest piece of experimental information that time. The total cross-sections were predicted to be a little lower than the observed ones [5]. For other reactions, *e.g.*, $pp \to pp\pi^0$, the discrepancies between the theory and experiment [7–14] were even larger.

It should be noted that the experimental data on the $pp \to pp\pi^0$ reaction near the energy of 1 Gev are much more scarce than those for the $pp \to pn\pi^+$ channel. The KEK data [10] contain the information on total cross-sections only. The only data on the spectra of secondaries at the energy 970 MeV were provided in the paper [8], the statistics being rather poor. For this reason it would be important to perform more accurate measurements of the cross-sections at this energy region and compare carefully

[a] e-mail: Victor.S@pnpi.spb.ru

Table 1. Numbers of events and cross-section values of the $pp \to pp\pi^0$ reaction.

P (MeV/c)	1581	1683
N_{events}	925	1087
$\sigma_{pp\pi^0}$ (mb)	4.19 ± 0.17	4.50 ± 0.17
$\sigma_{\text{exp}}/\sigma_{\text{OPE}}$	1.29 ± 0.05	1.31 ± 0.05

the differential distributions of the final particles in the $pp \to pp\pi^0$ reaction with the predictions of the modern OPE model. Such a comparison would allow one to see the strong and weak aspects of this simplest theoretical model, as well as to judge about the necessity of some additional nonperipheral mechanisms of the pion production in NN collisions. The results on the study of neutral pion production in the energy range below 900 MeV were published earlier in our work [11]. Here we present the results of the investigation of differential spectra and their comparison with the advanced OPE model [6] at two higher energies.

2 Experiment

The experiment was performed at the PNPI 1 GeV synchrocyclotron with the help of the 35 cm hydrogen bubble chamber disposed in the 1.48 T magnetic field. The proton beam (after the corresponding degrader for the momentum 1581 MeV/c) was formed by three bending magnets and by eight quadrupole lenses. The incident proton momentum value was inspected independently by the kinematics of the elastic-scattering events. The accuracy of the incident momentum value was about 0.5 MeV/c, the momentum spread being 25 and 7 MeV/c (FWHM) under 1581 and 1683 MeV/c, respectively. A total of 10^5 stereoframes were obtained at both proton momenta.

According to kinematics of the pion production in NN collisions, the laboratory angles of secondary protons are in the forward hemisphere, the maximum angle being not larger than 60° at our energies. For this reason we selected two-prong events with track angles in the plane of the film not larger than 60°.

The events selected so can belong not only to the neutral pion production but also to the elastic pp scattering or to the π^+ production reactions. The events in the fiducial volume of the chamber were measured and geometrically reconstructed. The identification of the events was performed on the strength of the χ^2 criterion, the confidence level being equal to 1%. If the event had a good χ^2 for the elastic version (4C-fit), it was considered as an elastic one. If several inelastic versions revealed a good χ^2, we used visual estimate of the ionization density to distinguish between the proton and pion.

The standard bubble chamber procedure was used to obtain absolute cross-sections [11]. Absolute values measured with the accuracy of about 4% are given in table 1 together with the statistics and ratios of experimental values to the OPE model predictions calculated here.

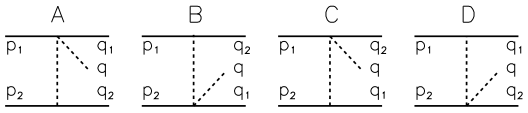

Fig. 1. Feynman diagrams of the OPE model for the $NN \to NN\pi$ reaction.

3 One-pion exchange model

According to the OPE model [1], the main role in the reaction $NN \to NN\pi$ is played by the pole diagrams (fig. 1). The matrix element of any diagram of fig. 1 can be presented as a product of three factors: the propagator, the amplitude of the πN scattering and the πNN vertex function

$$M_i \sim \frac{1}{k_i^2 + \mu^2} \Im(z_i, y_i^2; k_i^2) G(k_i^2), \tag{1}$$

where z_i is the total energy of the πN system, y_i^2 is the four-momentum transfer square in the πN scattering vertex, k_i^2 is the four-momentum square of the virtual pion and μ^2 is the pion mass squared.

The form factor function of the πNN vertex taking into account the nonpole diagram contributions was not determined in the frame of the OPE model. On the other hand, in [6] the following form was suggested for the form factor:

$$G(k_i^2) = \alpha\mu^2/[k_i^2 + (\alpha + 1)\mu^2]\,. \tag{2}$$

The choice of α in the range 8–9 gave a good description of the experimental data on the $pp \to pn\pi^+$ reaction in the energy range 600–1000 MeV.

The πN scattering amplitude $\Im(z_i, y_i^2; k_i^2)$ and its off-shell behaviour were taken according to [1], where the off-shell corrections were introduced into partial waves. We confined ourselves to the P_{33}-wave only in the partial-wave expansion, assuming the leading role of the Δ_{33}-resonance in the πN scattering. The partial off-shell f_{33} amplitude was taken in the form

$$f_{33}(z_i; k_i^2) = \Gamma(k_i^2) f_{33}(z_i; -\mu^2), \tag{3}$$

where $\Gamma(k_i^2)$ is the off-shell correction factor calculated in [1] in the frame of dispersion relations, while the on-shell partial f_{33} amplitude was taken in the Breit-Wigner form

$$f_{33}(z_i; -\mu^2) = \frac{1}{2b_i^s}\gamma[(z^* - z_i) - i\gamma/2]^{-1}\,, \tag{4}$$

with $\gamma = 2\gamma_0(ab_i^s)^3(1 + ab_i^s)^{-2}$, $z^* = 1232$ MeV, $a = 6.3 \times 10^{-3}$ MeV^{-1}, $\gamma_0 = 58$ MeV and b_i^s is the momentum of the proton scattered from a virtual pion.

The reaction matrix element is the sum of the matrix elements of the diagrams of fig. 1.

$$M = M_A - M_B - M_C + M_D\,, \tag{5}$$

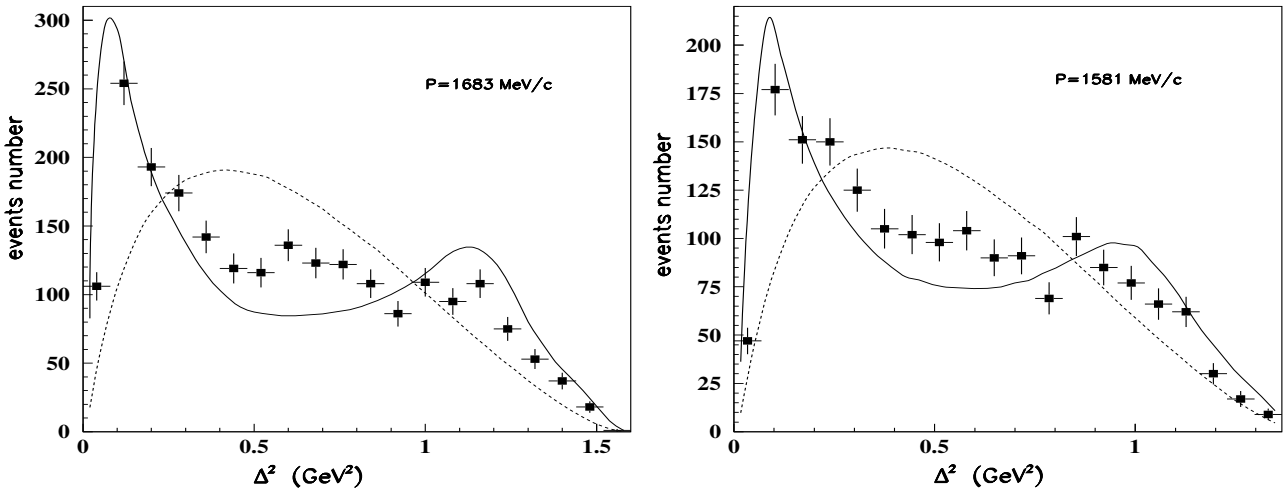

Fig. 2. The four-momentum transfer Δ^2 distributions. The solid and dotted curves are the calculations of the OPE model and the phase space, respectively, normalized to the total experimental number of events.

where the choice of signs is determined by the Pauli principle. All possible interference terms were taken into account. The details of the OPE model used here can be found in ref. [6].

We used a FOWL simulation program [15] in order to obtain all necessary distributions at once.

4 Experimental results and discussion

The main evidence for the pole diagram contribution would definitely be the observation of a peak in the momentum transfer distribution from the target particle to the secondary proton, (*e.g.,* for the diagram A, in the distribution on the $\Delta^2 = -(p_2 - q_2)^2$) at low momenta. But since there is no difference between the final protons in the $pp \to pp\pi^0$ reaction, it is difficult to separate the contribution of a certain diagram experimentally. The whole Δ^2 distribution is rather complex, because other diagrams have singularities on their own variables which spread the studied one. So the contribution of the diagram A really contains the low-momentum peak, while the B diagram contribution has a maximum at high Δ^2. It is quite natural because the diagram B has a singularity in $\bar{\Delta}^2 = -(p_1 - q_2)^2$ distribution, so for this diagram the beam proton is a spectator and Δ^2 is not small (p_2 is the nucleon mass in the laboratory system and q_2 is almost equal to p_1). The contributions of diagrams C and D are similar to those of B and A, respectively, but more spread out.

Figure 2 shows the Δ^2 distributions for our energies together with OPE model predictions (solid lines) and phase space calculations (dotted lines) normalized to the total experimental number of events, because the absolute values of the OPE model calculations do not agree with the experiment (see table 1). We shall return to this question later when we will discuss the energy dependence of the cross-sections.

Forgetting for a while the underestimated absolute cross-section values, we can see that the OPE model describes qualitatively well the data on Δ^2 at both energies studied. It is remarkable because one should bear in mind that only the P_{33}-wave was taken into account in the πN scattering.

Maybe, the Δ^2 distribution is mainly sensitive to the pole diagram propagator and the dependence on the πN amplitude manifests itself in other distributions.

Figure 3 presents the distributions in the momentum transfer from the beam proton to π^0-meson $r^2 = -(p_1 - q)^2$. Again one can see the qualitative agreement between the OPE calculations and the experimental data, though these distributions are less sensitive to the model since the phase space curves are also in reasonable agreement with the experiment. One can conclude that, at least from these data, the contribution of the nucleon exchange diagrams is rather small because the experiment does not reveal any peak at low r^2 as compared to the phase space.

One of the peripherality criteria of the interaction could be the isotropy of the Treiman-Yang angle distribution [16]. It should be isotropic if the process were determined by the exchange of a scalar particle (in our case, neutral pion). However, because of the indistinguishability of the final protons, (*e.g.,* for the diagram A one can take a q_1 proton from the πN scattering block instead of the q_2 proton) the final Treiman-Yang angle distribution will be distorted. For this reason, opposite to our previous work [11] we do not compare here the Treiman-Yang angle distribution with the OPE calculations.

Figures 4 and 5 show the laboratory momentum spectra of final protons and the pion of the $pp \to pp\pi^0$ reaction. In the proton spectra one can see two peaks, one in the region 300–400 MeV/c (independently of the incident energy) and the second moving to the left with the decrease of beam energy. The low-energy peak corresponds to the

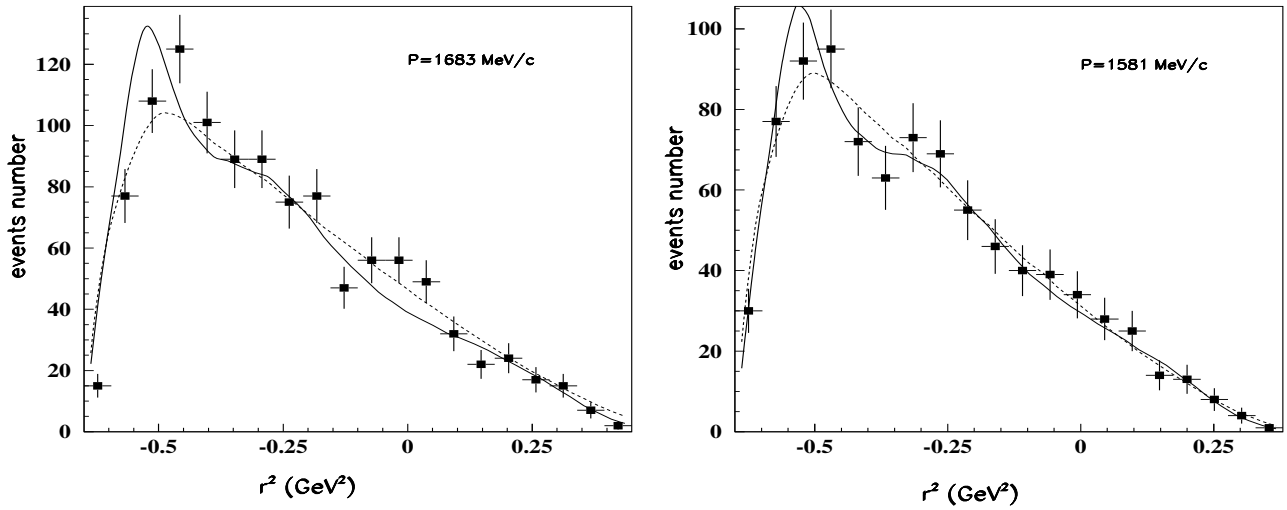

Fig. 3. The four-momentum transfer r^2 distribution. The curves have the same meaning as in fig. 2.

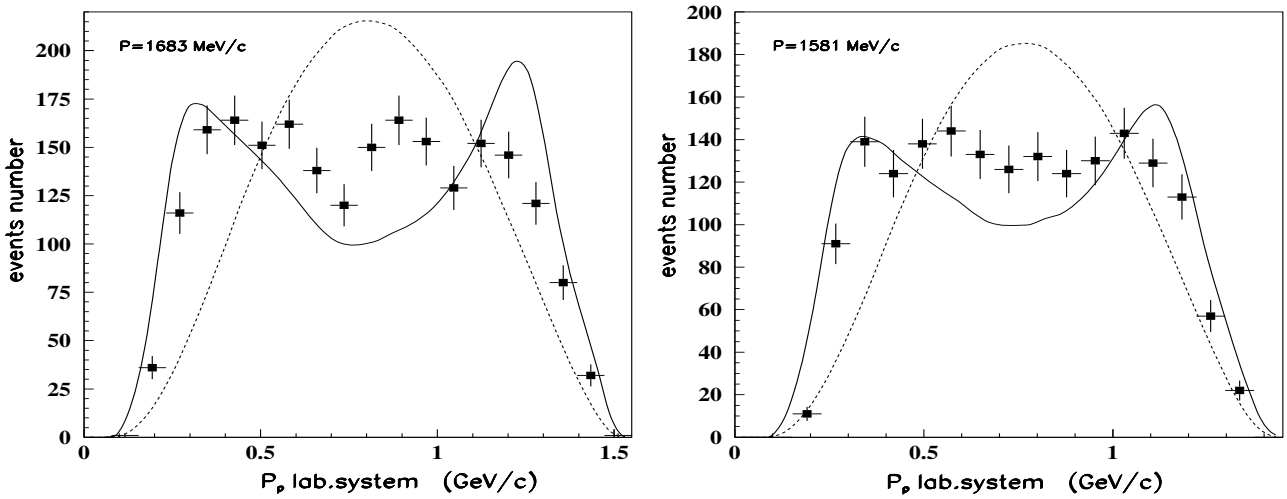

Fig. 4. The laboratory momentum spectra of the final protons. The curves have the same meaning as in fig. 2.

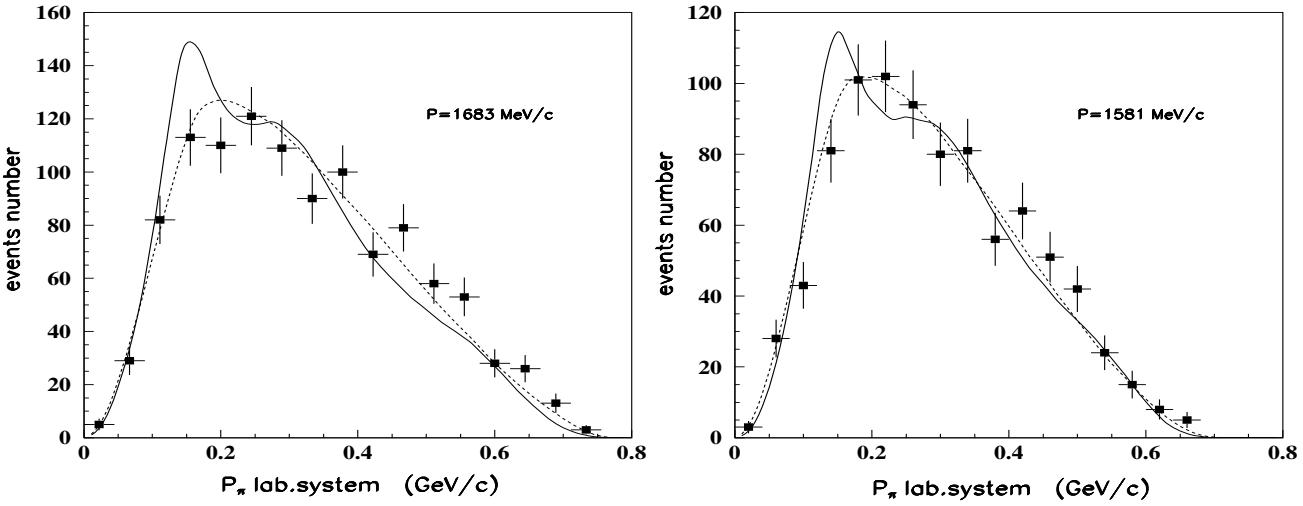

Fig. 5. The laboratory momentum spectra of π^0-mesons. The curves have the same meaning as in fig. 2.

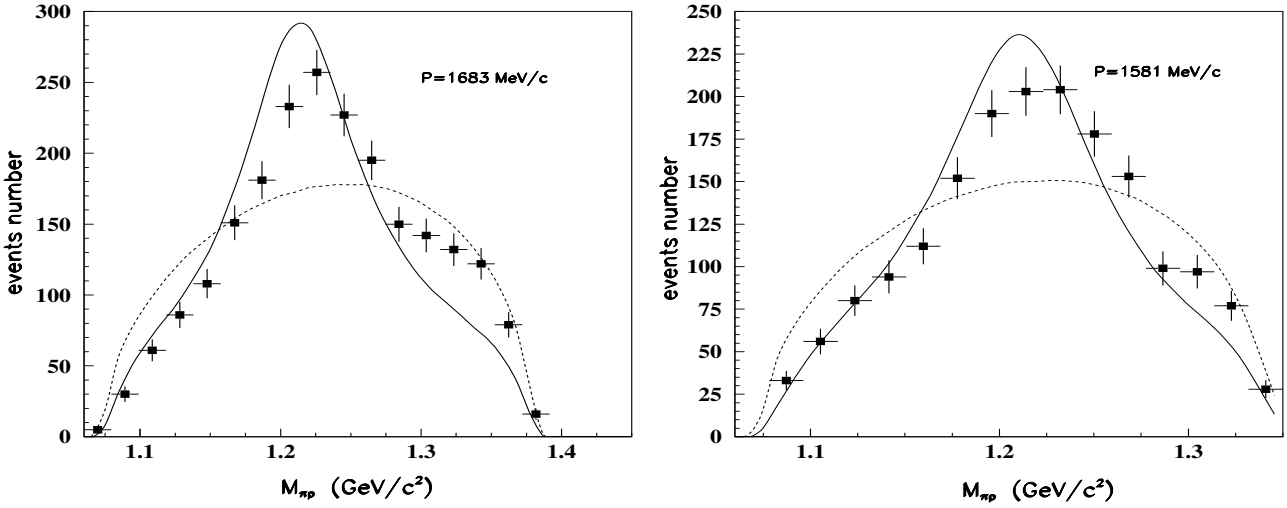

Fig. 6. $M_{p\pi^0}$ effective-mass spectra. The curves have the same meaning as in fig. 2.

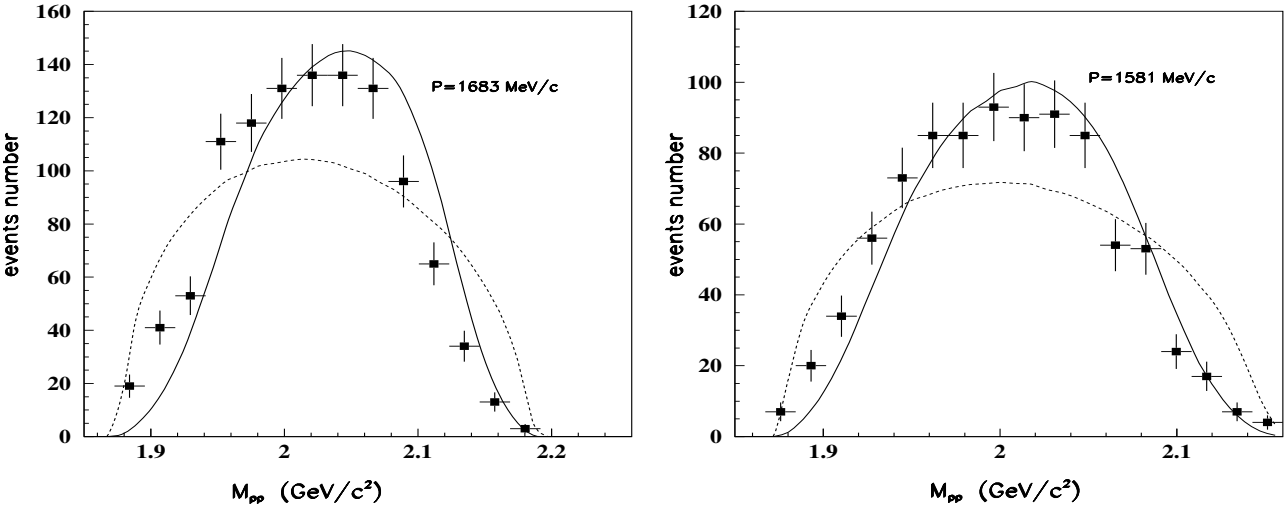

Fig. 7. Effective-mass spectra of final protons. The curves have the same meaning as in fig. 2.

target spectator proton, while the high-energy one corresponds to the incident proton being a spectator. The OPE calculations describe the experiment satisfactorily, contrary to the phase space ones. The pion spectra are close to the phase space distributions and are less representative.

Figures 6 and 7 show the $M_{p\pi^0}$ and M_{pp} effective-mass distributions. It looks like the distributions on $M_{p\pi^0}$ consist of two parts: one is the phase space distribution, while the other has the form of a peak with the width ~ 100 MeV/c^2. The peak location corresponds to the Δ_{33} mass. The origin of these two contributions is quite clear in the frame of the OPE model, if one keeps in mind that the πN scattering comes from the P_{33}-wave only. When the $M_{p\pi^0}$ is calculated for the spectator proton, (*e.g.,* q_2 in the diagram A, fig. 1) one has the phase space distribution. When the proton comes from the πN scattering block the resulting $M_{p\pi^0}$ distribution corresponds to the Δ_{33} isobar peak. As can be seen from figs. 6 and 7, OPE calculations are in qualitative agreement with the experiment at both energies studied. The same situation holds for centre-of-mass momentum spectra of pion and protons (figs. 8 and 9), and it is not a surprise because they connect one to one with the effective-mass distributions.

The c.m.s. angular distributions of protons are given in fig. 10. OPE calculations are in rather good agreement with the experimental data, with the exception for the small proton scattering angles. A possible explanation of this discrepancy is the presence of the sole P_{33}-wave in the πN scattering amplitude. It is clear that a small admixture of other waves interfering with the main one should manifest itself mainly in the angular distributions.

The angular distributions of pions together with OPE predictions are given in fig. 11. One should say that the distributions are far from being isotropic. Since the c.m.s. angular distributions of pions should be symmetrical, we

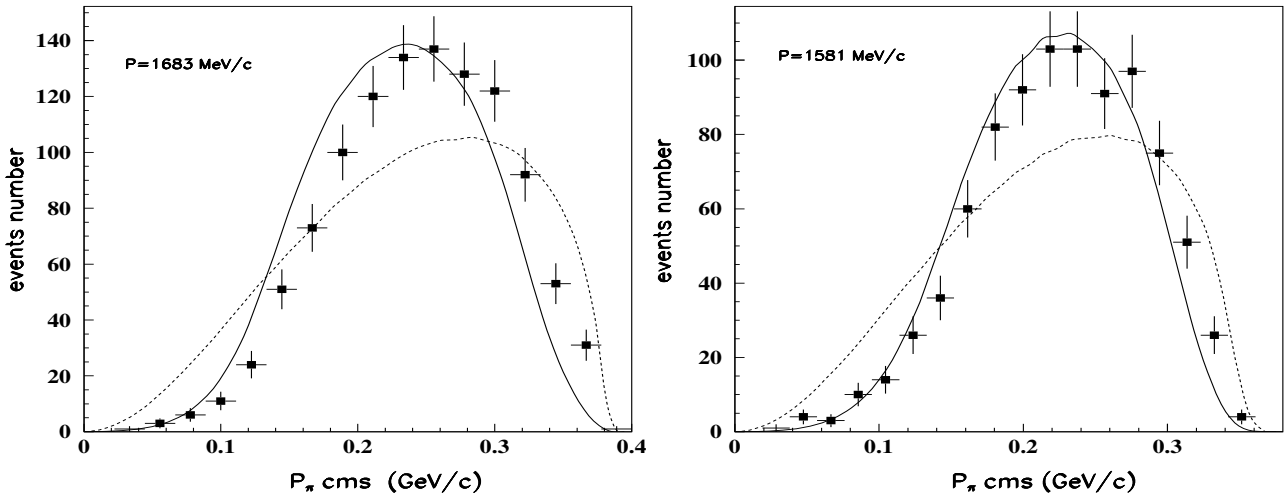

Fig. 8. Momentum spectra (c.m.s.) of π^0-mesons. The curves have the same meaning as in fig. 2.

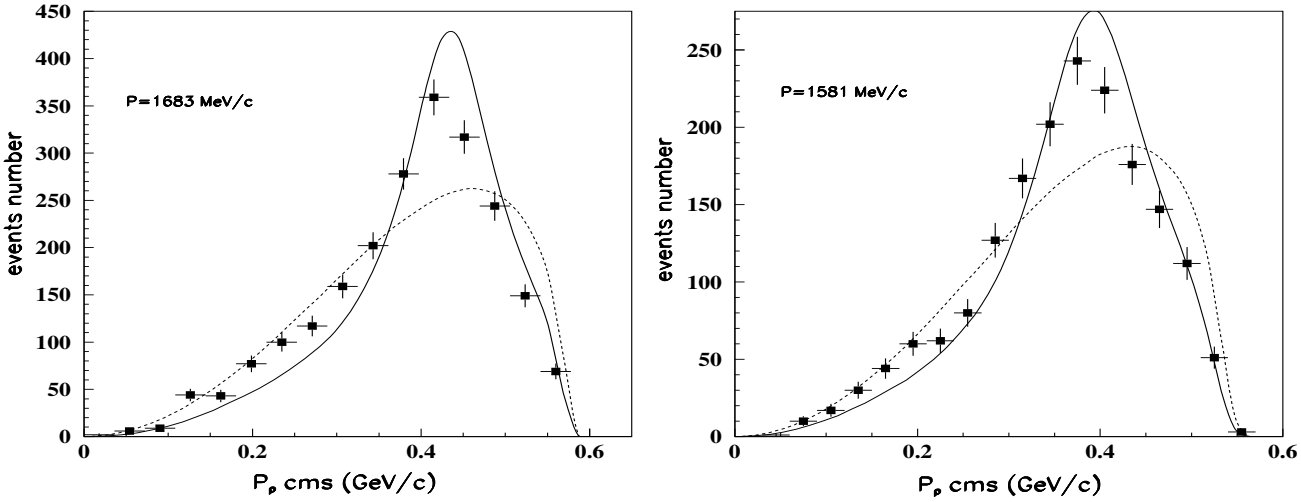

Fig. 9. Momentum spectra (c.m.s.) of final protons. The curves have the same meaning as in fig. 2.

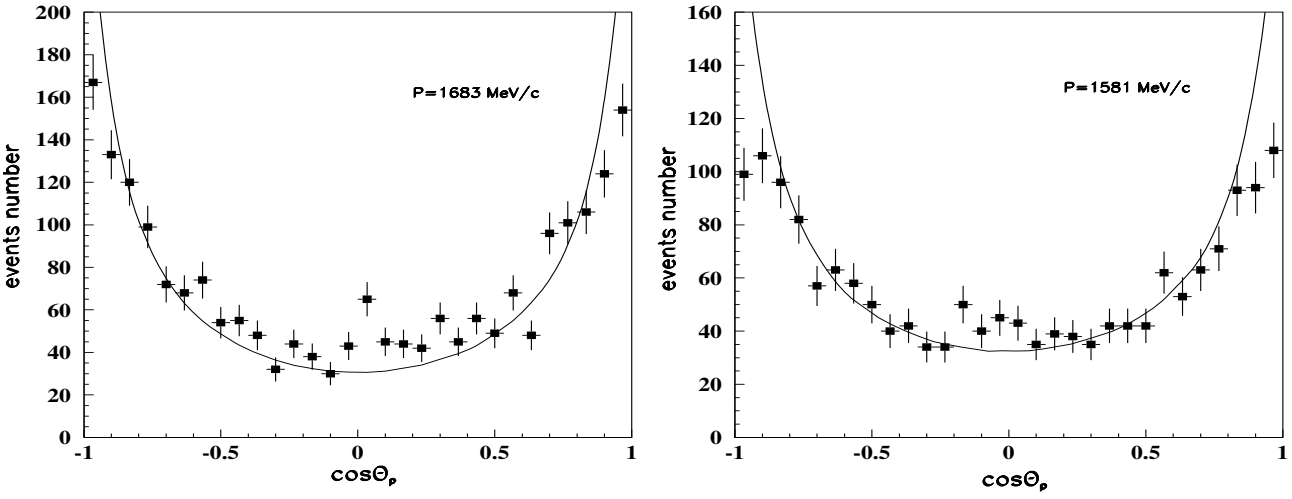

Fig. 10. Proton angular distributions (c.m.s.). The curves have the same meaning as in fig. 2.

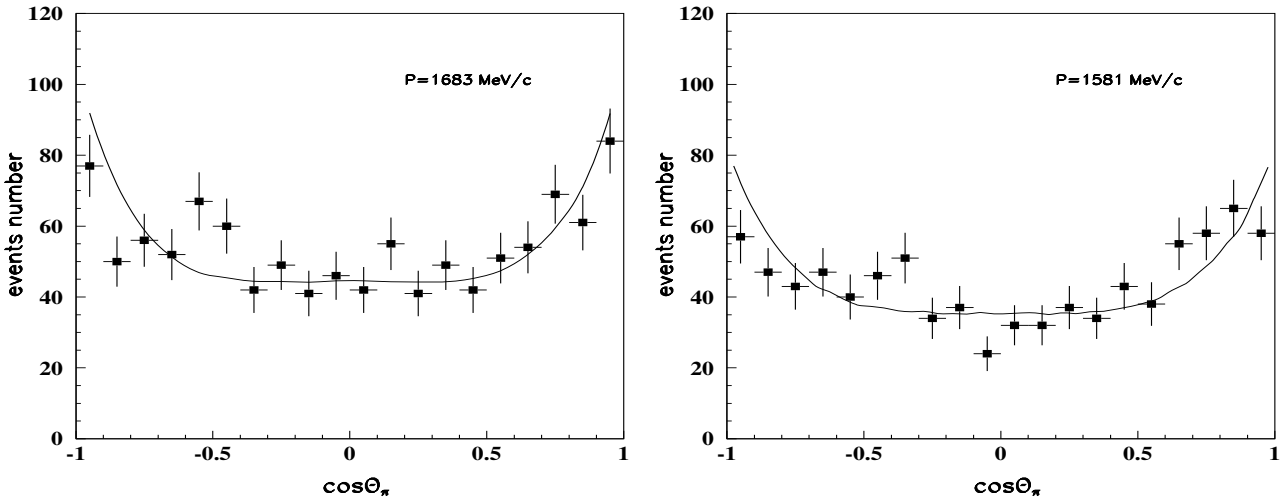

Fig. 11. π^0-meson angular distributions (c.m.s.). The curves have the same meaning as in fig. 2.

tried fitting to them by the formula

$$\frac{\mathrm{d}\sigma}{\mathrm{d}\Omega^*_{\pi^0}} \sim \frac{k}{2\pi}(1/3 + b\cos^2\theta^*_{\pi^0})\,. \qquad (6)$$

The results of such a fit are shown in fig. 12 together with the values found by other authors. The problem is important, being connected with the attempts to estimate the contribution from the isoscalar channel to the inelastic np interaction. If this contribution is zero, the angular distributions of charged pions in the $np \to pp\pi^-(nn\pi^+)$ reactions should be simular to those of π^0-mesons in the $pp \to pp\pi^0$ reaction. The presence of terms linear in $\cos\theta^*_{\pi^\pm}$ in the angular distribution of np reactions might be considered as an indication to the isoscalar contribution. It is clear that to catch a small contribution of the isoscalar channel one needs to know well enough a form of the isovector contribution for which the $pp \to pp\pi^0$ reaction provides better opportunity.

As is seen from fig. 12 the anisotropy factor b is rather badly determined and a scatter of values is fairly large. Nevertheless one can see that b increases gradually together with the energy and starting with the momentum of ~ 1.2 GeV/c it is in the range 0.2–0.4.

The OPE predictions for the opening angle of protons in c.m.s. do not differ much from the phase space descriptions and both agree with the experiment.

Figure 13 shows the distributions in $\cos\theta^*_{\pi^0 p}$ in c.m.s. The phase space description is in better agreement with the experiment than the OPE one at both energies.

The observation of narrow resonance peaks in the M_{pp} spectra in the reaction $np \to pp\pi^-$ was reported in [17], which were considered as candidates to the dibaryon resonances. Our effective-mass spectra M_{pp} (fig. 7) do not reveal any reliable evidences for such peaks.

We looked at M_{pp} distributions for the events with the cut in the momentum transfer from the incident proton to π^0-meson, the cut being similar to that used in [17], and again we did not observe any energy-independent peculiarities. Thus we failed to observe any evidence for narrow dibaryon resonances in the pp effective-mass spectra in the single-pion production. Still, it should be noted, that our resolution on two-proton masses is about 12 Mev/c^2 that is several times worse than that in the experiment [17]. Maybe, this is the reason why we do not resolve narrow structures observed in [17]. Nevertheless, if such peculiarities exist, they should be independent of the initial energy. It is interesting to look at the effective-mass distributions obtained by summing up the original ones at different incident momenta. In fig. 14 such distributions are shown

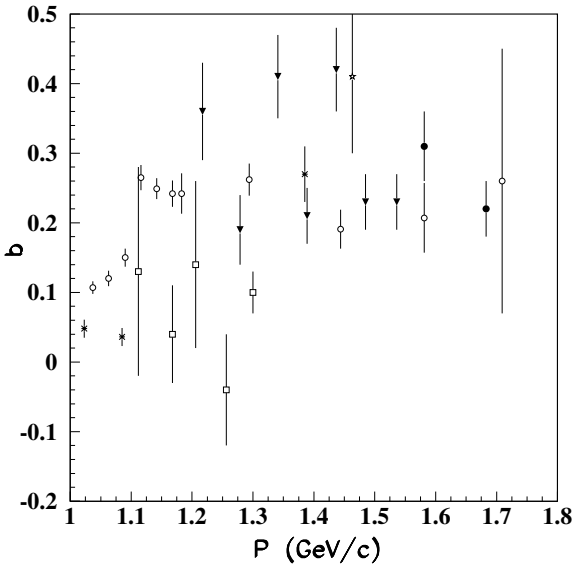

Fig. 12. The values of the parameter b from the fit of the angular distributions (c.m.s.) of the π^0-mesons according to the form $\frac{\mathrm{d}\sigma}{\mathrm{d}\Omega^*} \sim (\frac{1}{3} + b\cos^2\theta^*_{\pi^0})$. The data are from: this work (●), [7] (□), [9] (×), [11] (▼), [12] (∗), [13] (⋆), [14] (○).

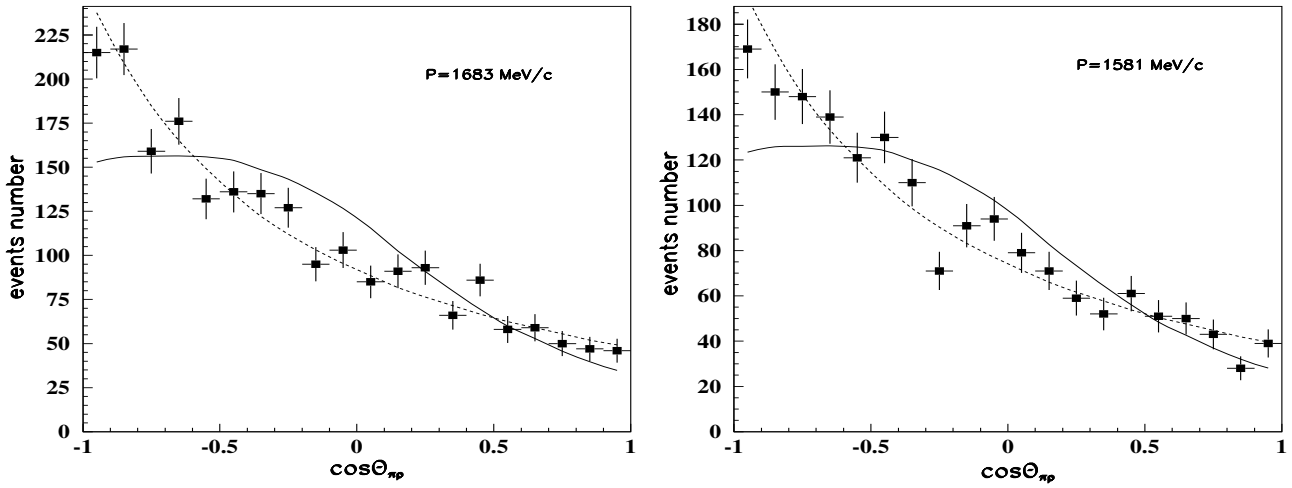

Fig. 13. Centre-of-mass opening angle distributions for proton and π^0-meson. The curves have the same meaning as in fig. 2.

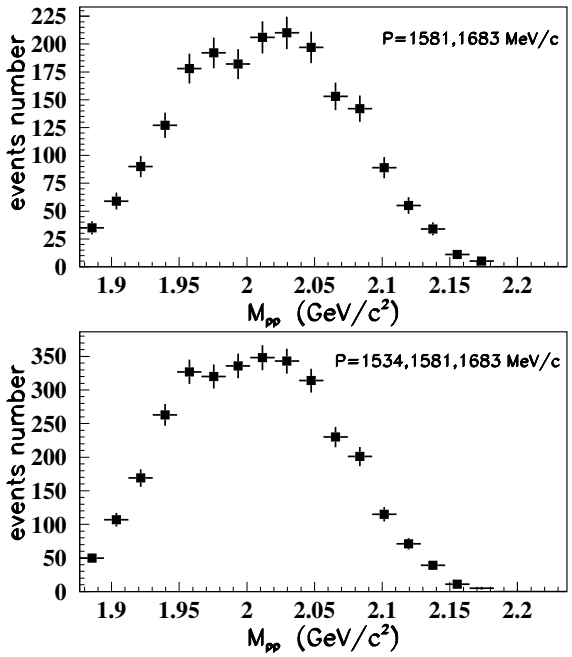

Fig. 14. The M_{pp} effective-mass spectra summing up on different incident momenta.

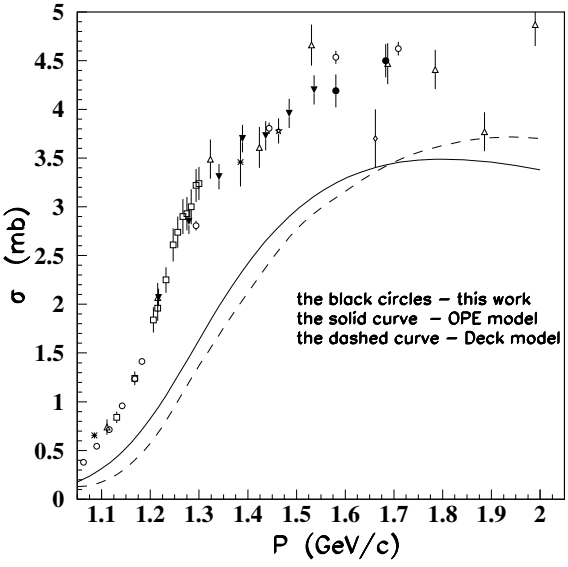

Fig. 15. Cross-section of the $pp \to pp\pi^0$ reaction. The solid curve is the OPE model calculation with the P_{33}-wave only. The dashed curve corresponds to Deck model calculations [6]. The data are from: this work (●), [7] (□), [8] (◇), [9] (×), [10] (△), [11] (▼), [12] (∗), [13] (⋆), [14] (○).

for two and three incident momenta (including the distribution at 1536 MeV/c from the work [11]). One can see some irregularities on the left-hand side of distributions in the range of the effective masses indicated for resonances in ref. [17].

As one can see in the above-given figures, there is a good qualitative agreement of the OPE model with experimental differential spectra while the predictions for the total cross-sections underestimate the data (see the third line of table 1). Why does the OPE model fail to describe the cross-section values for the $pp \to pp\pi^0$ reaction? The existing experimental data on the total cross-sections are shown in fig. 15 together with the model predictions. It is seen that there is an obvious discrepancy between the OPE model calculations (solid curve) and experimental cross-sections. One can obtain better agreement with a proper choice of form factor, but such a choice destroys the agreement with total cross-sections of the $pp \to pn\pi^+$

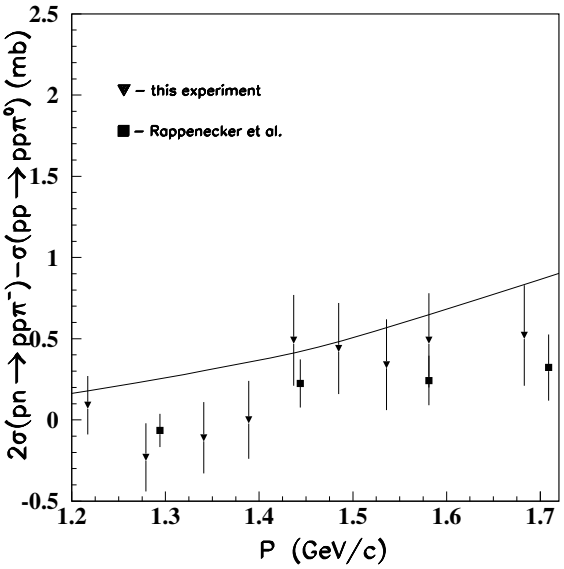

Fig. 16. Isoscalar inelastic cross-section. The curve is the calculation of the Deck model [5].

reaction, as was shown in ref. [11]. One might guess that the reason for such a situation is that the πN amplitude is not good enough because only the P_{33}-wave was taken into account. The dashed curve in fig. 15 corresponds to the predictions of the Deck model [5], where the πN vertex includes all the waves obtained in the phase shift analysis [18]. One can see that this does not change the situation significantly. One should keep in mind, however, that, with an exception for the P_{33}-wave, there is no good prescription for the calculation of the off-shell correction, being very important as can be seen for the P_{33}-wave [19]. So the question is still open.

The present measurements together with our previous data at lower energies [11] as well as measurements of cross-sections of the $pn \to pp\pi^-$ reaction [20] allow one to obtain the energy dependence of the isoscalar inelastic cross-section

$$\sigma(I=0) = 3[2\sigma(np \to pp\pi^-) - \sigma(pp \to pp\pi^0)] \ . \qquad (7)$$

Figure 16 shows one third of the isoscalar inelastic $NN\pi$ cross-section at energy points where we have measured the $pp \to pp\pi^0$ reaction (triangles) together with the points of ref. [14] (squares). The values of $\sigma(np \to pp\pi^-)$ were obtained by the interpolation to the same final kinetic energy in the c.m. system. It is worth noting that the observed behaviour of the cross-section is like the solution B of Bystricky *et al.* [21]. One can see that the isoscalar cross-section is close to zero up to the momentum 1.4 GeV/c, and furthermore it rises in agreement with the prediction of the Deck model [5] (solid curve).

5 Conclusions

A detailed study of differential cross-sections of the $pp \to pp\pi^0$ reaction has been performed at two incident energies near 1 GeV. The shape of the distributions is described by the OPE model quite well, in spite of the fact that the P_{33}-wave only is used in the πN scattering amplitude. Certain distributions (for example, in figs. 4 and 13) do not agree well with the OPE calculations, that may indicate to some other mechanisms contributing to the single-pion production. However, this mechanism does not manifest itself in other differential distributions.

On the other hand, the OPE model fails to predict the correct total cross-sections and it cannot be helped by the simple choice of the form factor.

The study of the effective-mass spectra gives no convincing evidence for the existence of narrow dibaryon resonances. We can conclude that, if such a six-quark system exists, it represents, most probably, a small admixture in the nuclear matter. Recall that such candidates to dibaryon resonances were observed in the reaction with light nuclei [22].

We would like to express our gratitude to the bubble chamber staff as well as to the laboratory assistants, which toiled at the film scanning and measuring. A half of the measurements of selected two-prong events at one momentum was carried out on the "Elit" device in the Institute of Nuclear Physics of Moscow State University. We would like to express our deep acknowledgement to Prof. P.F. Ermolov for supporting this work as well as to N. Grishin and the staff of engineers of the INP MSU without whom this work could not be completed. The authors thank L.G. Dakhno for careful reading of the manuscript and useful remarks.

References

1. E. Ferrary, F. Selleri, Nuovo Cimento **27**, 1450 (1963); **21**, 1028 (1961); F. Selleri, Nuovo Cimento A **40**, 236 (1965).
2. I.P. Auer *et al.*, Phys. Rev. B **67**, 113 (1977).
3. B. Tatischeff *et al.*, Phys. Rev. C **59**, 1878 (1999).
4. B.J. Ver West, Phys. Lett. B **83**, 161 (1979).
5. A. König, P. Kroll, Nucl. Phys. A **356**, 345 (1981); W. Jauch, A. König, P. Kroll, Phys. Lett. B **143**, 509 (1984).
6. V.K. Suslenko, I.I. Gaisak, Yad. Fiz. **43**, 392 (1986).
7. A.F. Dunaitsev, Y.D. Prokoshkin, Zh. Eksp. Teor. Fiz. **36**, 1656 (1959) (Sov. Phys. JETP **9**, 1179 (1959)).
8. D.V. Bugg *et al.*, Phys. Rev. **133**, 1017 (1964).
9. R.J. Cence *et al.*, Phys. Rev **131**, 2713 (1963).
10. F. Shimizu *et al.*, Nucl. Phys. A **386**, 571 (1982).
11. V.P. Andreev *et al.*, Phys. Rev. C **50**, 15 (1994); V.P. Andreev *et al.*, Z. Phys. A **329**, 371 (1988).
12. S. Stanislaus *et al.*, Phys. Rev. C **44**, 2287 (1991).
13. C. Comptour *et al.*, Nucl. Phys. A **579**, 369 (1994).
14. G. Rappenecker *et al.*, Nucl. Phys. A **590**, 763 (1995).
15. F. James, CERN program library, Th68-15 (1968).
16. E. Ferrari, Phys. Lett. **2**, 66 (1962).
17. Y.A. Troyan, V.N. Pechenov, Sov. J. Nucl. Phys. **56**, 191 (1993).

18. G. Höhler *et al.*, *Handbook of Pion-Nucleon Scattering*, Fachinformationszentrum, Karlsruhe, Phys. Data **12-1** (1979).
19. V.K. Suslenko *et al.*, JINR preprint **P2-88-113**, Dubna, 1988, unpublished.
20. L.G. Dakhno *et al.*, Phys. Lett. B **114**, 409 (1982).
21. J. Bystricky *et al.*, J. Phys. (Paris) **48**, 1901 (1987).
22. L.V. Fil'kov *et al.*, Eur. Phys. J. A **12**, 369 (2001).